

Intelligent Water Drops with Perturbation Operators for Atomic Cluster Optimization

R.M. Gamot, P.M. Rodger

Centre for Scientific Computing, University of Warwick
r.m.gamot@warwick.ac.uk, p.m.rodger@warwick.ac.uk



Overview

The Intelligent Water Drops algorithm was modified (MIWD) and adapted to allow it to determine the most stable configurations, for the first time, of Lennard-Jones (LJ), Binary LJ (BinLJ), Morse and Janus Clusters. The algorithm, referred as MIWD+PerturbOp, is an unbiased type of algorithm where no *a priori* cluster geometry information and construction were used during initialization. Cluster perturbation operators were applied to clusters generated by MIWD to further generate lower energies. A limited-memory quasi-Newton algorithm, called L-BFGS, was utilized to further relax clusters to its nearby local minimum.

Basic Properties of IWD

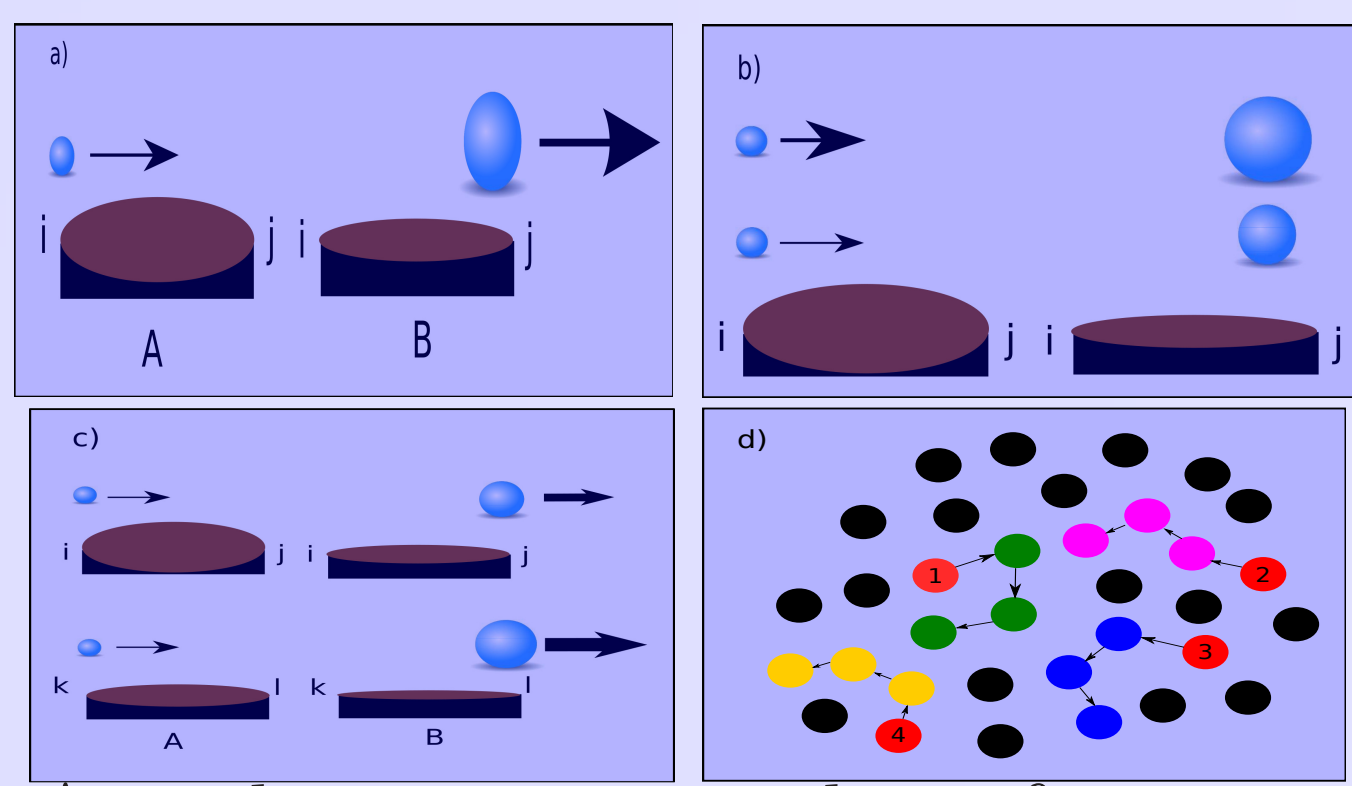
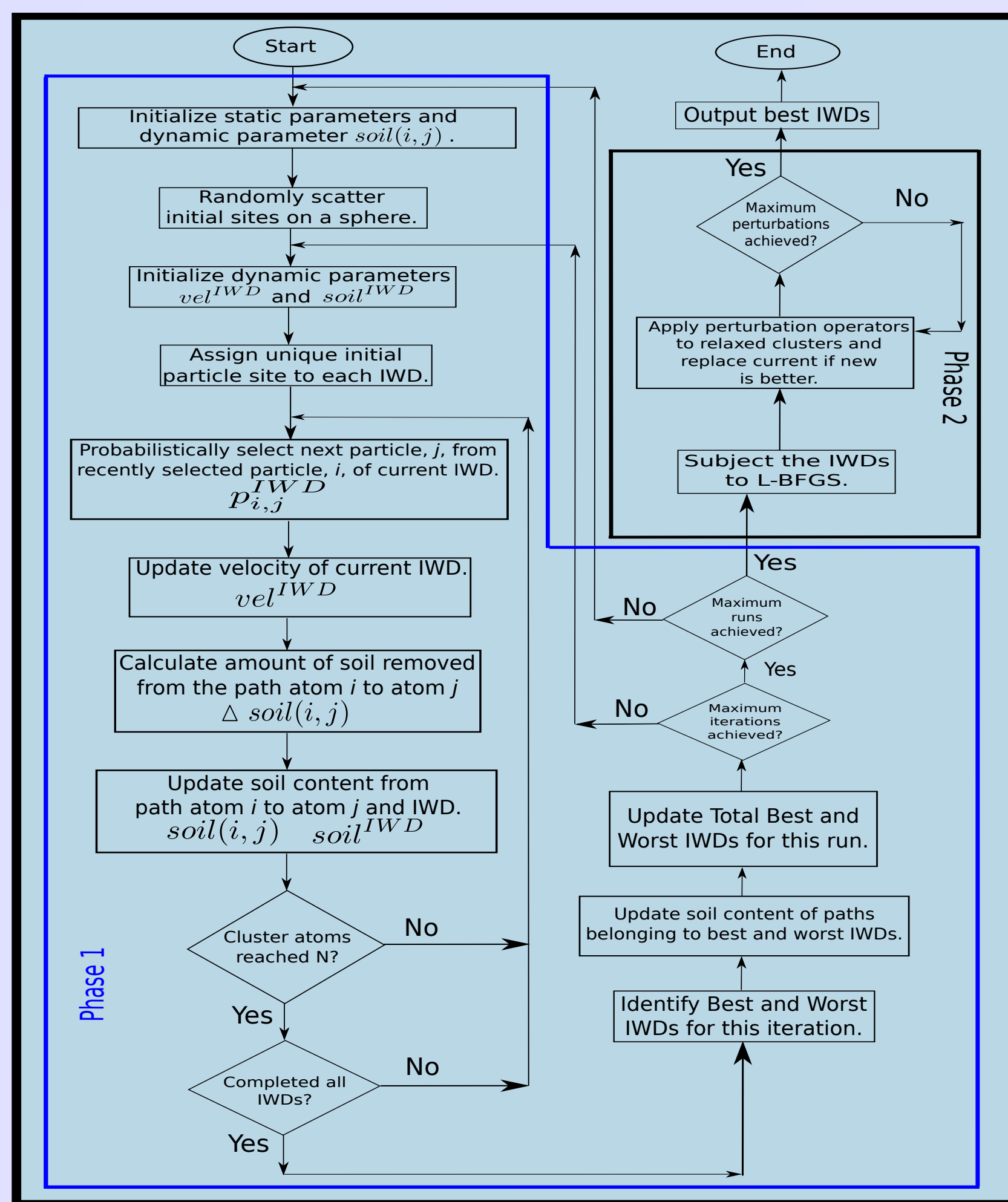


Figure 1: A path measures quality of connectivity between particles. (a) An IWD gathers soil (brown ellipse) as it flows from particle i to particle j while $path(i,j)$ loses an amount of soil; (b) Soil gathered increases with IWD velocity; (c) An IWD travelling on a path with lesser soil, $path(m,n)$, will gather more soil and higher velocity. (d) The algorithm progressively builds the cluster by choosing the connectivity with desirable measures.

FlowChart of MIWD



Modifications to IWD

- The probability of choosing a path depends on amount of soil and the potential energy.

$$p_{i,j}^{IWD} = \frac{f(soil(i,j))\eta(i,j)}{\sum_{k \in V_{IWD}} f(soil(i,k))\eta(i,k)}$$

$$\eta(i,j) = \frac{1}{2 + V_{type}(r_{i,j})}$$

$$V_M = e^{a(1-r_{i,j})} (e^{a(1-r_{i,j})} - 2)$$

$$V_{LJ}(r_{i,j}) = 4\epsilon_{i,j} \left(\left(\frac{\sigma_{i,j}}{r_{i,j}} \right)^{12} - \left(\frac{\sigma_{i,j}}{r_{i,j}} \right)^6 \right)$$

$$V_J(r_{i,j}) = V_{LJ}(r_{i,j}) f(\Omega_i) f(\Omega_j)$$

$$f(\Omega_i) = -\exp\left(\frac{\theta_{i,j}^2}{2\sigma^2}\right) + \exp\left(\frac{(\theta_{i,j}-180)^2}{2\sigma^2}\right)$$
- An appropriate heuristic undesirability factor, HUD , is chosen to fit atomic cluster optimization.

$$HUD_{i,j} = \eta(i,j)^{-1} + \mu r_{i,j} + \beta (\max(0, r_{i,j}^2 - D^2))^2$$
- Worst iteration agent, TIW , affects the soil content as well.

$$soil(i,j) = (1 + \rho)soil_{i,j} + \rho \left(\frac{soil^{IWD}}{N-1} \right)$$
- L-BFGS was used as a relaxation algorithm for IWDs.

Acknowledgements

Study is funded by Warwick Chancellor's Scholarship (formerly WPRS) and Centre for Scientific Computing. Computing facilities are provided by the Centre for Scientific Computing of the University of Warwick with support from the Science Research Investment Fund. RMT Gamot is also supported by the University of the Philippines (UP) System under the UP Doctoral Studies Fund.

On LJ Clusters

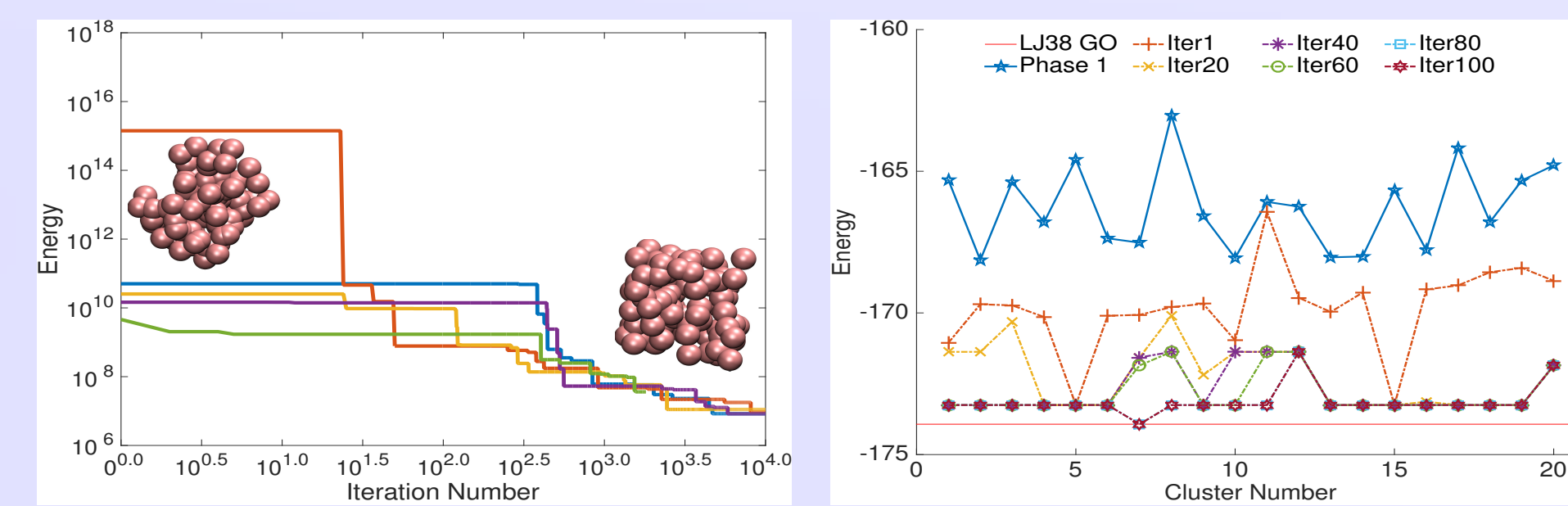


Figure 2: Left : Five independent LJ_{98} test runs (color lines) (10,000 iterations/run) showing decline in cluster energy. Right : Cubic Bounding volume and Grow Etch perturbation operator shows energy decline as tested on LJ_{38} .

Runs of MIWD alone show improvement as iterations progress. Energies of the final runs for MIWD+GrowEtch, utilizing spherical bounding volume for scattering of initial sites, agree exactly with CCD (Cambridge Cluster Database) results up to $N = 104$ atoms. Compactness measures (Fig. 3) of this study versus CCD results show high-accuracy. Rotation and translation reveal that chiral clusters were generated. MIWD+GrowEtch achieved relatively high-success rates for difficult clusters compared to Basin-Hopping (BH), Basin-Hopping with Occasional Jumping (BHOJ) and Parallel Fast Annealing Evolutionary Algorithm (PFAEA) (Table 1).

Cluster Size	MIWD+PerOp	BH	BHOJ	PFAEA
38	100%	87%	96%	39%
75	50%	1%	5%	1%
76	20%	5%	10%	4%
77	10%	6%	5%	2%
98	75%	10%	10%	4%
102	5%	3%	16%	9%
103	40%	3%	13%	10%
104	15%	3%	12%	7%

Table 1: Good success rates with all "difficult" LJ clusters.

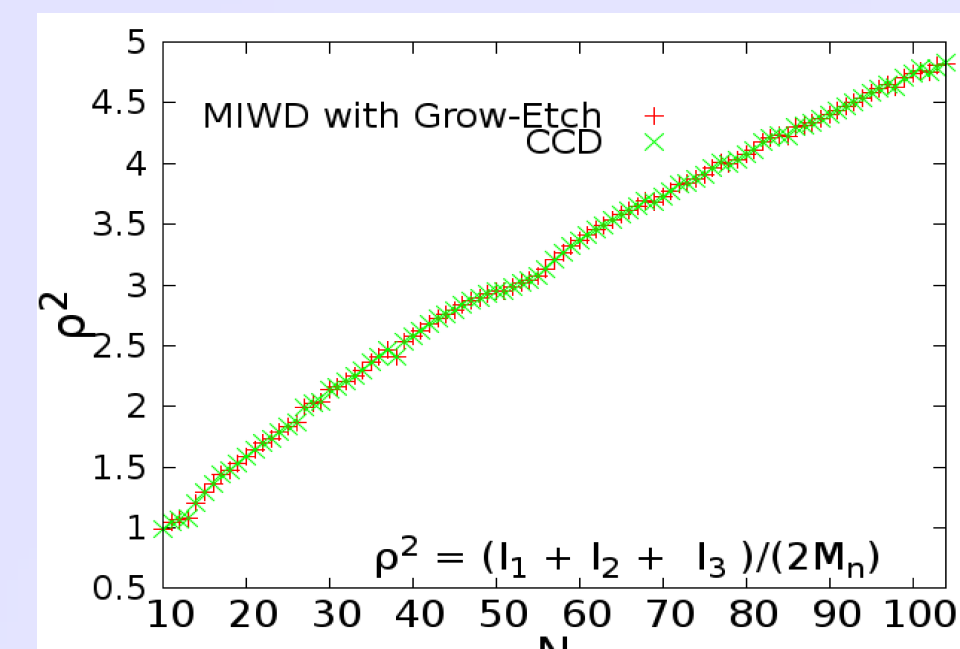


Figure 3: Compactness of clusters MIWD+GrowEtch versus CCD.

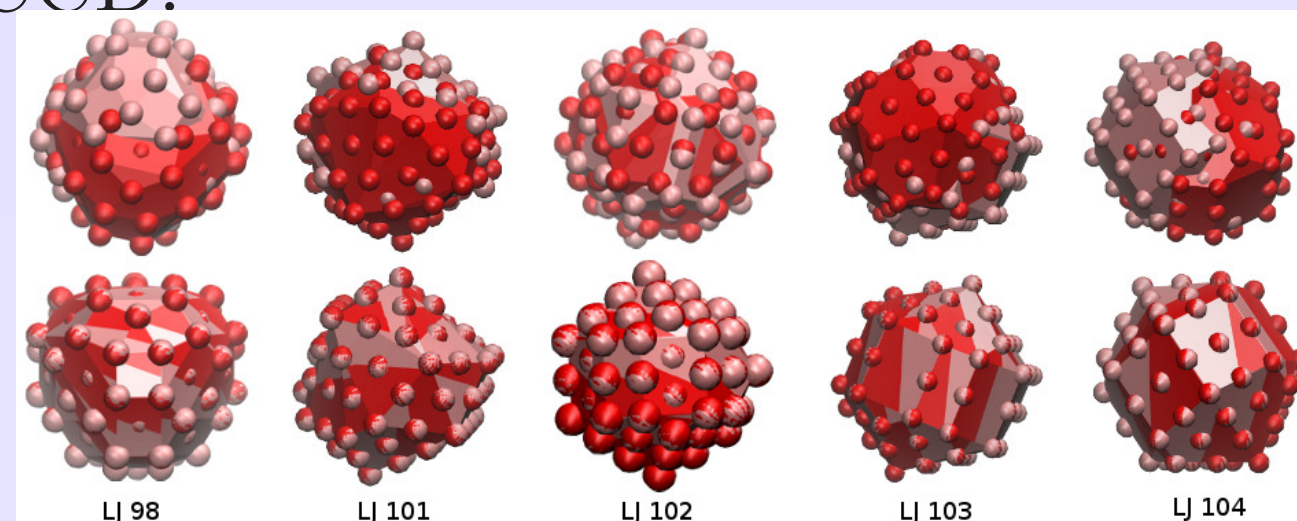


Figure 4: Row 1 : Overlaid clusters showing unmatched positions. Row 2 : Rotated and translated clusters showing matching configurations.

On Binary LJ and Morse

BINARY LJ : Tested for up to 50 atoms on 6 instances of $\sigma_{BB} = 1.05 - 1.30$. MIWD+Knead rediscovered the global minima (GM) for most of the clusters except for $N = 41, 43, 45-49$ for $\sigma_{BB} = 1.05$ and $N = 46, 47$ for $\sigma_{BB} = 1.10$. MIWD+CutSpliceVar rediscovered most of the GM except for $N = 35-36, 39-50$ for $\sigma_{BB} = 1.05$, $N = 46-47, 49-50$ for $\sigma_{BB} = 1.10$, $N = 35$ for $\sigma_{BB} = 1.15$, and $N = 30-32$ for $\sigma_{BB} = 1.30$. Combination of perturbation operators (CombiOp) in Phase 2 (CutSplice+Knead, CutSplice+H1L2, CutSplice+H2L1, Knead+H1L2 and Knead+H2L1) were further done. Combinations were able to arrive at the GM except for $N = 41, 43, 45, 46, 48, 49$ for $\sigma_{BB} = 1.05$ and $N = 46$ for $\sigma_{BB} = 1.10$.

MORSE : Tested for up to 60 atoms on 2 values of interparticle force range ($a = 6, 14$). MIWD+GrowEtch located the GM for most of the clusters except for $N = 47, 55, 57, 58, 60$ for $a = 14$.

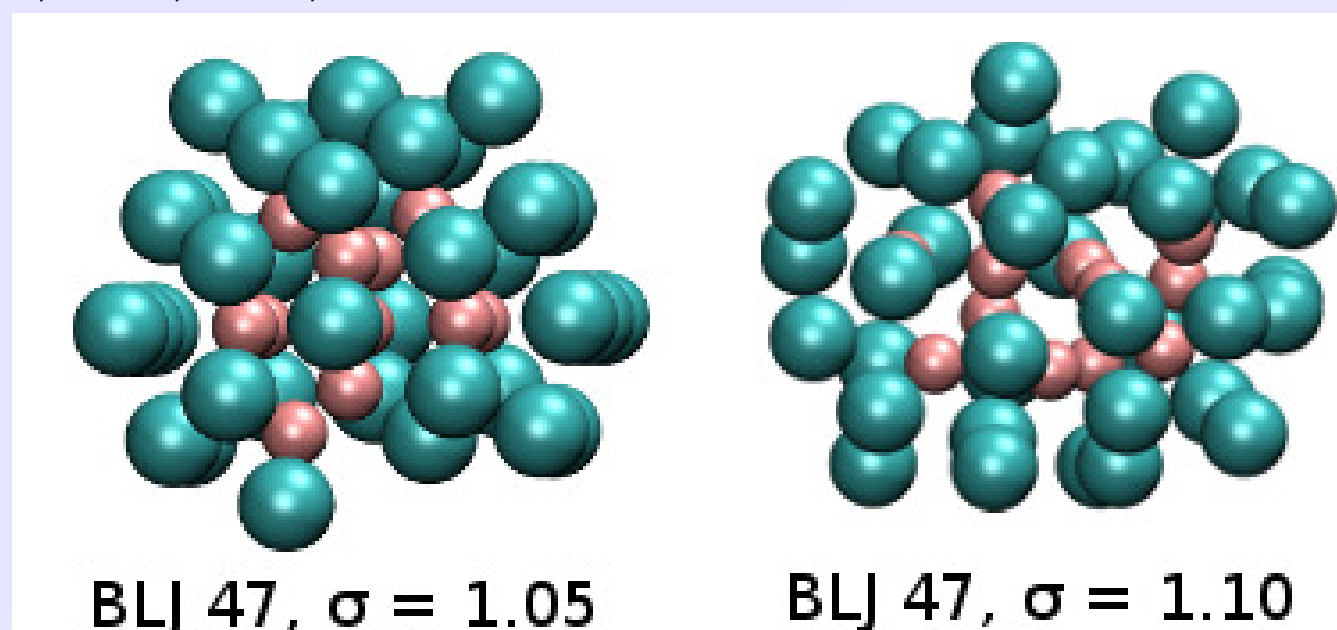


Figure 5: GM configurations generated from MIWD+CombiOp for selected Binary LJ Clusters.

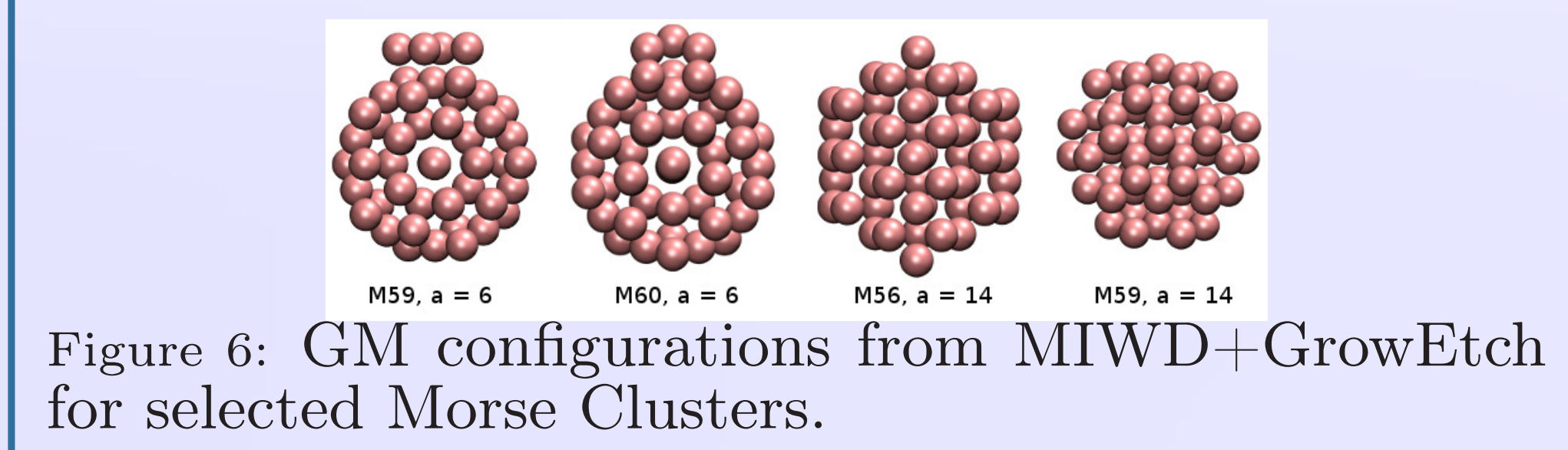


Figure 6: GM configurations from MIWD+GrowEtch for selected Morse Clusters.

On Janus Clusters

MIWD+CombiOp was applied on Janus clusters using the LJ potential as the patchy particles model but where anisotropic attraction and repulsion is modulated by an orientational dependent term MV_{ang} (Fig. 7). Configurations were predicted for cluster sizes $N = 3 - 50$ and $N = 100$. MIWD with GrowEtch and Patch Orientation Mutation produced the configurations with the lowest energies.

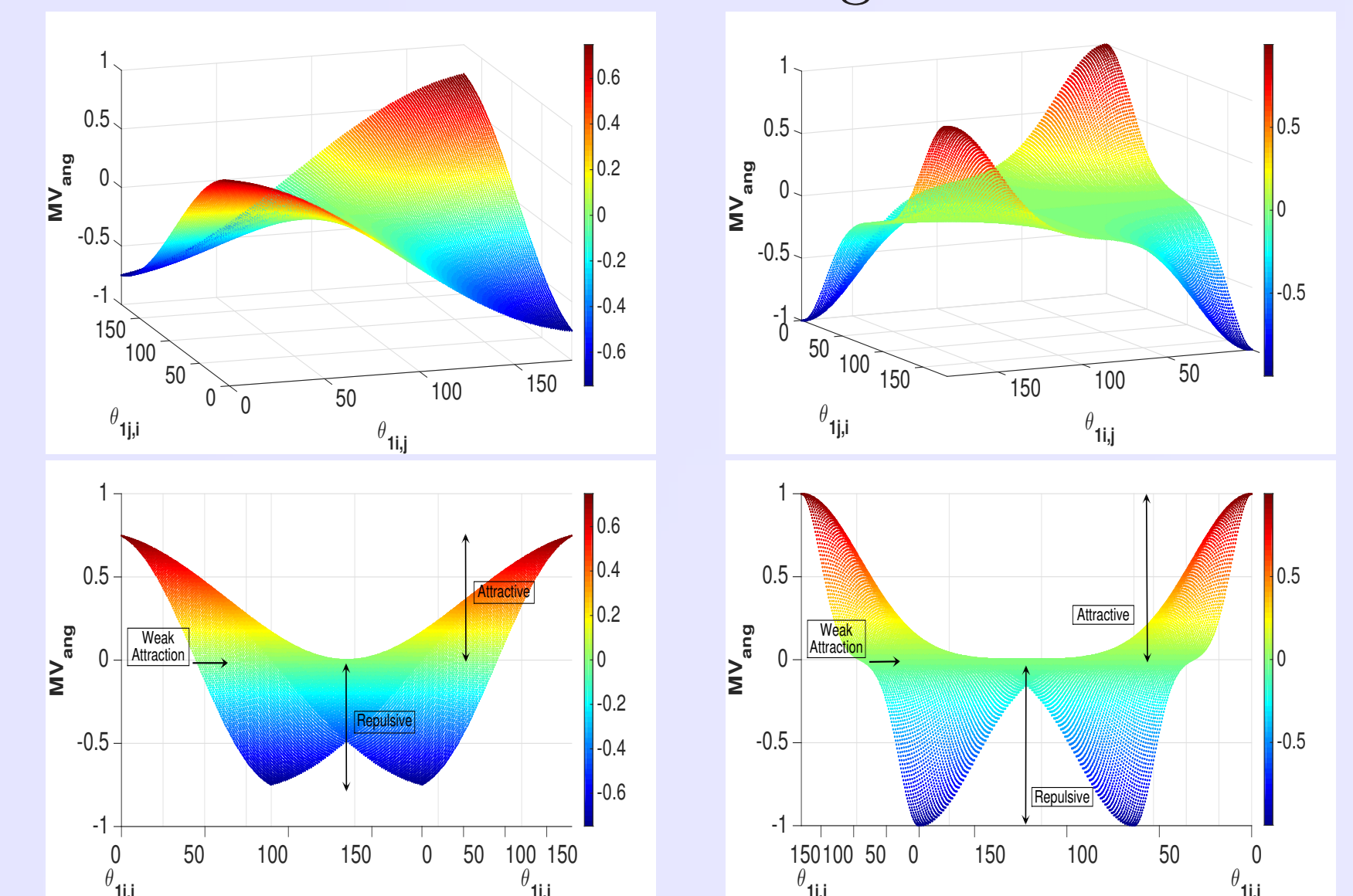


Figure 7: Orientation interaction, MV_{ang} , for pairs of angles between 0° to 180° . MV_{ang} for $\sigma = 90$ (Column 1) and $\sigma = 30$ (Column 2).

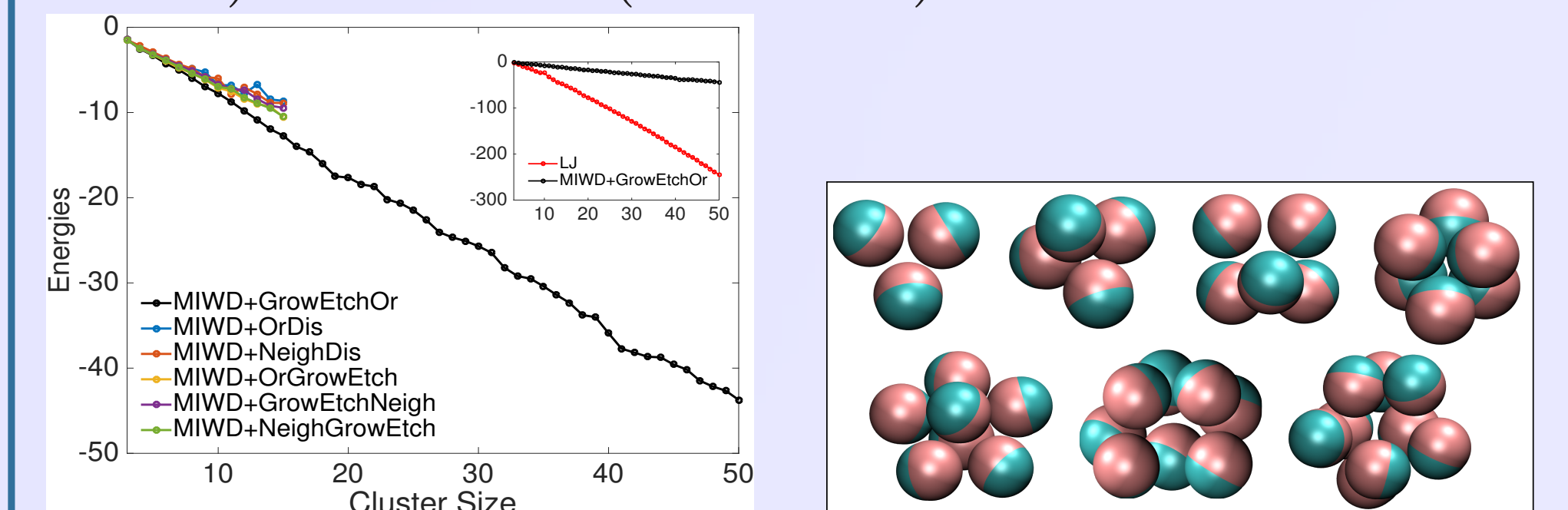


Figure 8: Left : Lowest Cluster Energies generated by MIWD+CombiOp for Janus clusters sizes $N = 3 - 50$. Right : Observed basic structures in Janus Clusters.

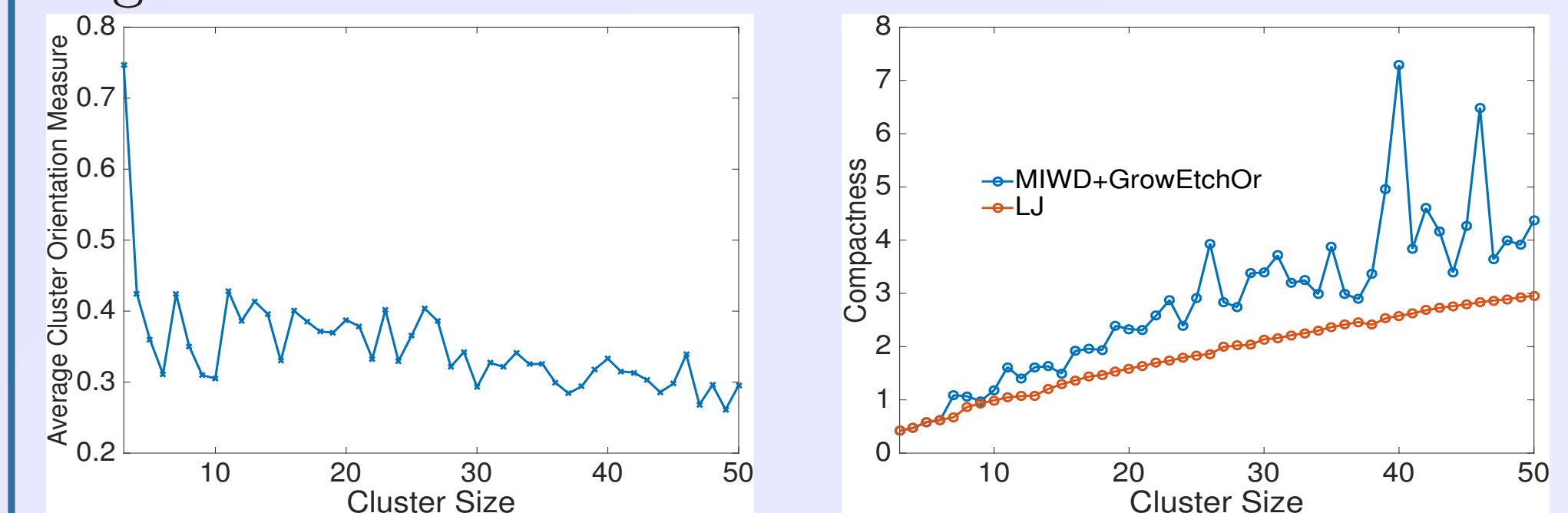


Figure 9: Left : Average orientation measure of each Janus particle with its neighbouring particles. Right : Compactness of Janus clusters compared to global optima LJ clusters.

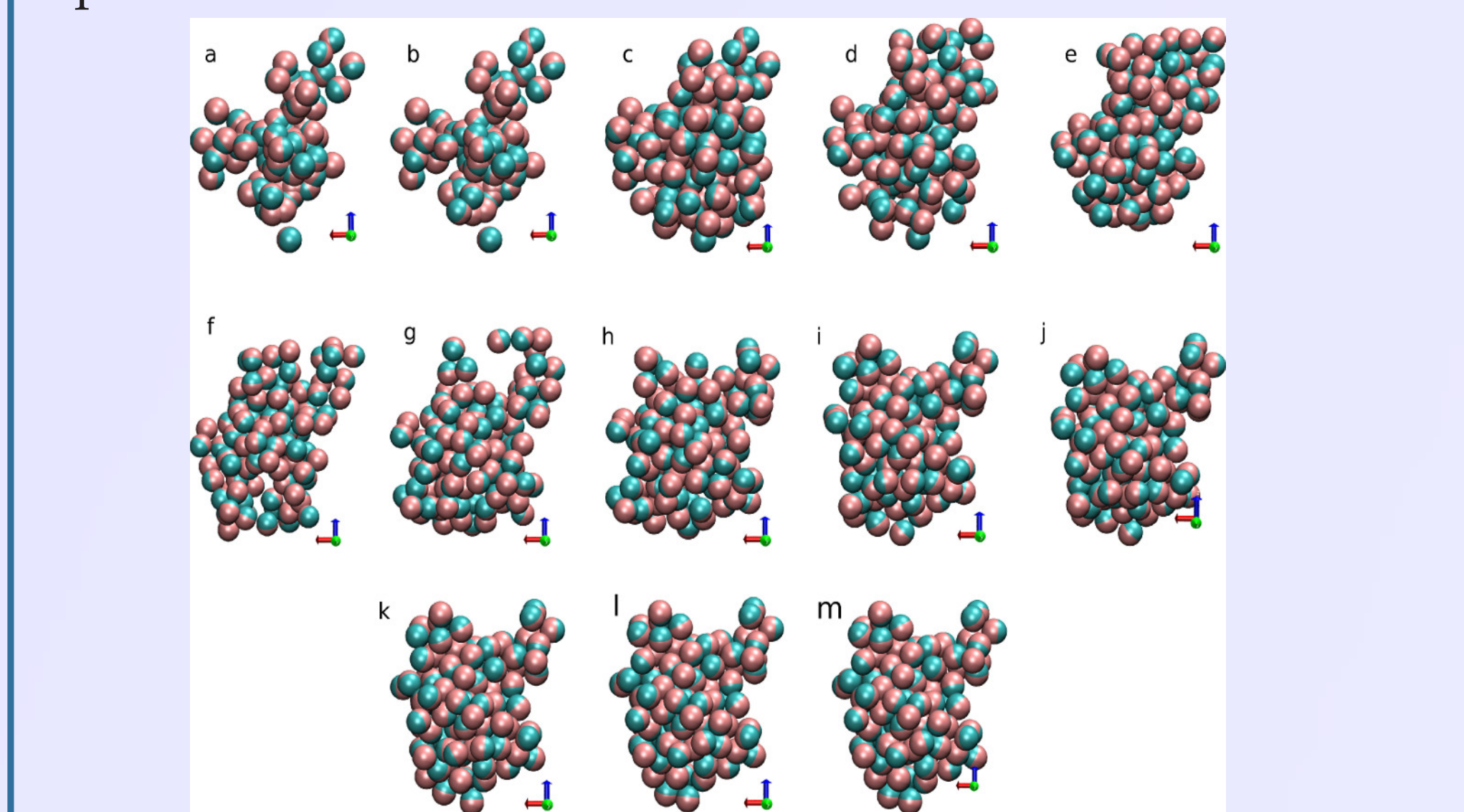


Figure 10: Snapshots from iterations of MIWD+CombiOp for J_{100} . Geometries in a and b are from Phase 1 while structures obtained from d to m are Phase 2 results. Geometry in c is the relaxed configuration resulting from Phase 1.

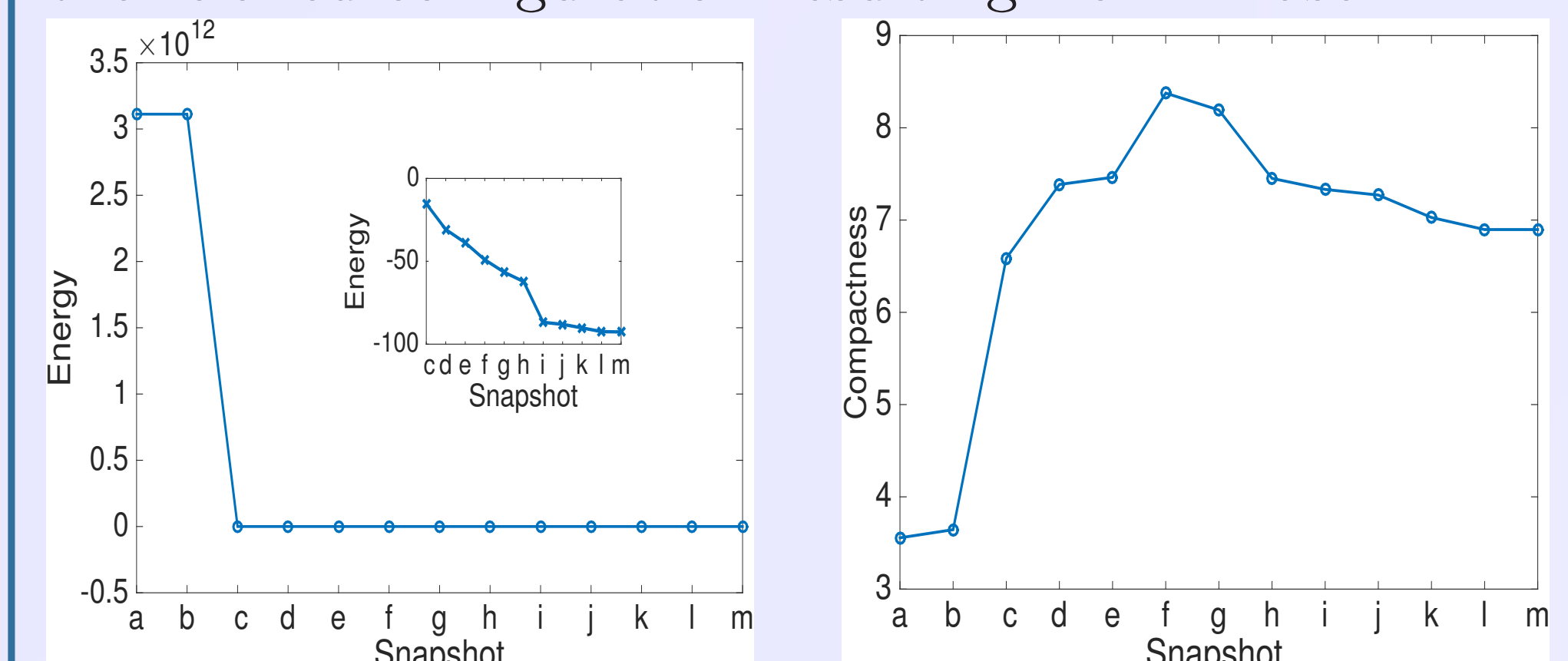


Figure 11: Left : Energies of Janus configurations in snapshots a to m . Right : Compactness of configurations in snapshots a to m .